Cleaner Materials 1 (2021) 100018

Contents lists available at ScienceDirect

Cleaner Materials

journal homepage: www.elsevier.com/locate/clema

Functionalization of tannic acid and campesterol with polyelectrolyte multilayer membranes for lithium ions separation and recycling

P. Nikhil Chandra [a,b,*], Kishore Kumar Nair [c]

[a] Department of Chemistry, Sree Narayana College, Kollam, Kerala 691001, India
[b] Advanced Centre of Environmental Studies and Sustainable Development, Mahatma Gandhi University, Kottayam 686560, India
[c] University of Free State, Bloemfontein 9301, South Africa

ARTICLE INFO

Keywords:
Lithium
Membranes
Ultrafiltration
Macromolecules
MIUF
MEUF

ABSTRACT

The potential use of chitosan/poly(styrene sulfonate) (CHS/PSS) polyelectrolyte multilayer (PEM) membranes functionalized with tannic acid (TA) and campesterol (CHT) for efficient separation and recycling of lithium from aqueous matrix under ultrafiltration conditions are examined. The PEM assembled via layer by layer (LbL) method accelerates the recycling process of lithium as it efficiently separates the metal complexed larger molecules. A total of eight CHS/PSS bilayers were sufficient for the effective lithium recovery. The microscopic studies confirmed the surface morphological change of PEM from smooth to rough after immobilization (MIUF). The successful immobilization of TA and CHT into PEMs are illustrated using spectroscopic studies. The TA and CHT assisted separation (MEUF) are also carried out by complexation of metal solution prior to filtration. The assisted mode provides a very good recovery of >94% with a excellent permeate flux of 1.25 m^3/m^2 day and 1.96 m^3/m^2 day for TA and CHT respectively. The recycling of lithium ions from water matrix is experimented with different parameters and experimental conditions. The reusability and extended life of the membrane systems indicate its potential in small scale filtration units.

1. Introduction

Lithium has been proved to contain characteristics like high electrochemical activity, high specific heat capacity, and a low thermal expansion coefficient, which make it an excellent candidate for various modern industrial applications (Xu et al., 2021). As a result, lithium and its compounds have been widely applied in commercial fields which rapidly raised the demand for lithium in recent years (Battistel et al., 2020). As per the latest US Geological Survey (U.S. Geological Survey, 2020), about 65% consumption of lithium belongs to batteries manufacture and about 20% belongs to ceramics and glass industry and the rest includes industries like alloys, medicine, lubricants, polymer industries, air treatment and so on. The global demand for lithium resources has risen in the last two decades due to the wide spread use of lithium ion based batteries in vehicle industry, telecommunication devices and other large scale energy storage applications (Lv et al., 2020). To meet this increasing demand, it is necessary to improve the production line as well as the existing recycling technology available for lithium. Also, if disposed improperly, the spent lithium ion batteries have also become a serious environmental concern. They can be hazardous due to the toxic and flammable fluorine containing organic electrolyte and several heavy metals present in it (Chen et al., 2015). Even though its availability in nature is very much lesser than its current demand, the need for lithium is expected to grow steeply in the coming years as lithium based batteries are going to power most of the future electric and hybrid vehicles (Ciftci and Er, 2015). Lithium batteries include both lithium ion and lithium polymer batteries with future technologies like lithium-sulfur or lithium-air types. These huge requirements must be satisfied from its available sources like ores and brines. Thus, the market will require an increased requirement with twice to six times the capability of its mineral sources (Wang et al., 2006).

Electric vehicles that use rechargeable lithium batteries have lower operating costs and zero emissions into the atmosphere will effectively reduce greenhouse gases owing toward a low carbon energy future (Dewulf et al., 2010). The isolation, reuse and recycling of renewable green energy lithium metal ions is, therefore, critical for a sustainable development of the world. Non renewability of lithium mines, geological imbalances, and increase in battery price underline the significance of the development of an innovative protocol for its recovery

* Corresponding author at: Department of Chemistry, Sree Narayana College, Kollam, Kerala 691001, India.
E-mail address: nikhilchandrap@snckollam.ac.in (P. Nikhil Chandra).

https://doi.org/10.1016/j.clema.2021.100018
Received 28 July 2021; Revised 29 August 2021; Accepted 1 September 2021

(Kang et al., 2013). About 2 billion lithium ion based batteries with an average life time of 2 or 3 years were sold every year, which usually end up in local land fill or incinerator (Xu et al., 2008). The stricter environmental regulations have prompted society to look for technical alternatives in order to treat these types of residues since the consumption of batteries is considerable around the world. At the same time, the increasing levels of metal ions in the drinking water represent a serious threat to human health and ecological systems (Nikhil et al., 2018).The lithium removal/recovery technologies from aqueous streams still have many draw backs, the main drawback being energy intensiveness. Metal ions separation techniques like precipitation, electro deposition, liquid–liquid extraction, evaporation, adsorption, ion exchange and crystallization were found to be effective but possess several disadvantages like time consuming, high operational cost, lack of easiness, use of high amount of solvents, low efficiency at low metal concentration etc (Jha et al., 2020). The higher loss percentage of lithium ions in these processes is also a problem, which advocates improving the current recycling strategies. Again, the indiscriminate leaching behavior of lithium and available complex separation process with high cost and potential heavy metal containing hazard emission, weakened many separation techniques. An effective separating process would be more suitable for recycling the used lithium ion batteries. From the point of view of selectivity and efficiency, separation of lithium ions from solutions by using polymeric membranes is an important way of approach to solve the existing problem.

The polyelectrolyte multilayer membranes (PEM's) find a large number of applications in selective ion transport, metal recovery, electronics, biosensors and water purification (Nikhil and Mothi, 2020). Low pressure filtration method like ultrafiltration (UF) is quite often viewed as purely size based separation but can also be extended for the removal of low molecular weight compounds and ions with surface modification. Preparation of composite membranes by surface coating using LbL (layer by layer) method on microfiltration membrane could upgrade its filtration properties from molecular level (Chandra and Usha, 2021). The flexibility of the polyelectrolyte skin in its morphology, thickness and permeation characteristics would make it an economical and aqueous based cleaner technology. The performance of PEM's can be further enhanced with macromolecule immobilized ultrafiltration (MIUF) method. In MIUF, suitable macromolecules are immobilized within PEM's to convert it into a framework composite membrane system capable of efficient complexation with lithium ions. Another possibility is the macromolecule enhanced ultrafiltration (MEUF) method. In MEUF, suitable macromolecules with anionic interactive sites can bind to lithium ions which are positively charged. Further, this can be ultrafiltered through PEM membranes whose pore size is now much smaller than the complexed metal ion to reject more efficiently. Lithium ions adsorbed and complexed with macromolecules are rejected subsequently. The permeation quality is good to be reused and the concentrations of the macromolecules and the lithium ion are high in the retention and the volume of the retention is much smaller than that of the stock used, so the retention is easier to be further treated, such as recycling the macromolecules and lithium. This method is of some advantages such as simple operation, high removal efficiency, metal ion recycle.

In the current MIUF and MEUF studies, the removal efficiency of lithium ions and impacts of some parameters on these methods are also studied. The studies proved to check the practicability and potential of these methods into practical application. The focus of these experiments is to design, investigate MIUF and MEUF filtration processes with characterization of PEM membranes and to compare two filtration processes. The effects of some important parameters were investigated, including number of bilayers, macromolecule concentration, solution pH, make up salt and effect of surfactant with a check on its self life and reusability. In this study, two macromolecules tannic acid (TA) and campesterol (CHT) were used in the MIUF and MEUF process to study their effect on the removal of lithium ions from water.

2. Experimental and methods

2.1. Materials

The supporting membranes used were Ultipor N66 microfiltration membranes (0.45 μm pore size, nylon 66) procured from Pall Life Sciences. The polyelectrolytes used for bilayer fabrication were chitosan (CHS, medium MW, 75–85 % deacetylated) and poly(styrene sulfonic acid) sodium salt (PSS, MW ~ 200,000, 30 wt% in water) acquired from Aldrich. Tannic acid (TA, MW ~ 1701, T8406, Sigma-Aldrich) and campesterol (CHT, MW ~ 400, Sigma-Aldrich) were used as complexing agents in MIUF and MEUF experiments. Other reagents included lithium ion standard (1000 ppm, Aldrich), NaCl (Merck), sodium dodecyl sulfate (SDS) (Merck), HCl (Merck), and NaOH (Merck) were used without further purification. Ultrapure water (Milli-Q, 18.2 MΩ cm, Pall Corporation) was used for membrane rinsing and preparation of polyelectrolyte and feed solutions.

2.2. PEM membrane fabrication and MIUF experimental setup

The PEM fabrication was achieved by LbL (layer by layer) method which includes alternative immersion of membranes on oppositely charged aqueous polyelectrolyte at room temperature. The ultipore supporting membrane was kept in ultrapure water for 24 h. For the sequential adsorption of the layers, the supporting membrane was first immersed in the solution of the cationic polyelectrolyte (CHS, 0.02 M, pH 1.7), rinsed with deionized water, then immersed in the solution of the anionic polyelectrolyte (PSS, 0.02 M, pH 1.7), followed by rinsing with water. Immersion time in the individual polyelectrolyte solution was kept as 15 min. By repeating the procedure for desired number (2 to 8 bilayers) of CHS/PSS nano bilayered PEM's were obtained. The macromolecule TA was prepared at pH 9.0 ($pK_a \sim 6$) to ensure its functional group activeness with three different concentrations. The TA solutions were always prepared in fresh before experiments and stored in the dark at 4 °C to prevent any further decomposition (Cruz et al., 2000). The CHT at three different concentrations were also prepared at slightly acidic pH by mixing the desired amount and stirring in water for two hours for its complete dissolution and then filtered (Sorenson and Sullivan, 2007). The different concentration of tannic acid (TA) and campesterol (CHT) were utilized to prepare the framework composite membrane system for MIUF experiments. The modified composite membranes were washed and dried thoroughly to ensure correct binding and repeatability.

2.3. MIUF and MEUF methods

Lithium stock solution was measured and added accurately into the deionized water to produce the synthetic stock solution with Li^+ concentration of 10^{-3} mol/L. The MIUF and MEUF experiments were carried out in a batch stirred cell (Amicon 8400 stirred cell, Millipore), at room temperature. The stirring speed was maintained constant at 400 rpm to obtain effective agitation and vortex approximately one third of the depth of the liquid for uniform filtration. The pH range of the feed solutions was set between 5.8 and 6.6. The applied transmembrane pressure (pressure drop across the membrane) of 20 psi at room temperature was achieved by nitrogen gas. The feed volume was 100 cm^3 and the ultrafiltration experiments were carried out until 50 cm^3 of the total sample was filtered. The permeate solution flux was calculated by measuring the volume of permeate collected with effective membrane area, and the sampling time. A schematic diagram of ultrafiltration with two modes was given in Fig. 1. In MIUF method, the complexation of macromolecule with lithium metal ions is occurred via solid phase, which is embedded between PEM's of composite membrane system. In MEUF, the complexation is expected via liquid phase by all intermolecular forces, mainly ionic or complex

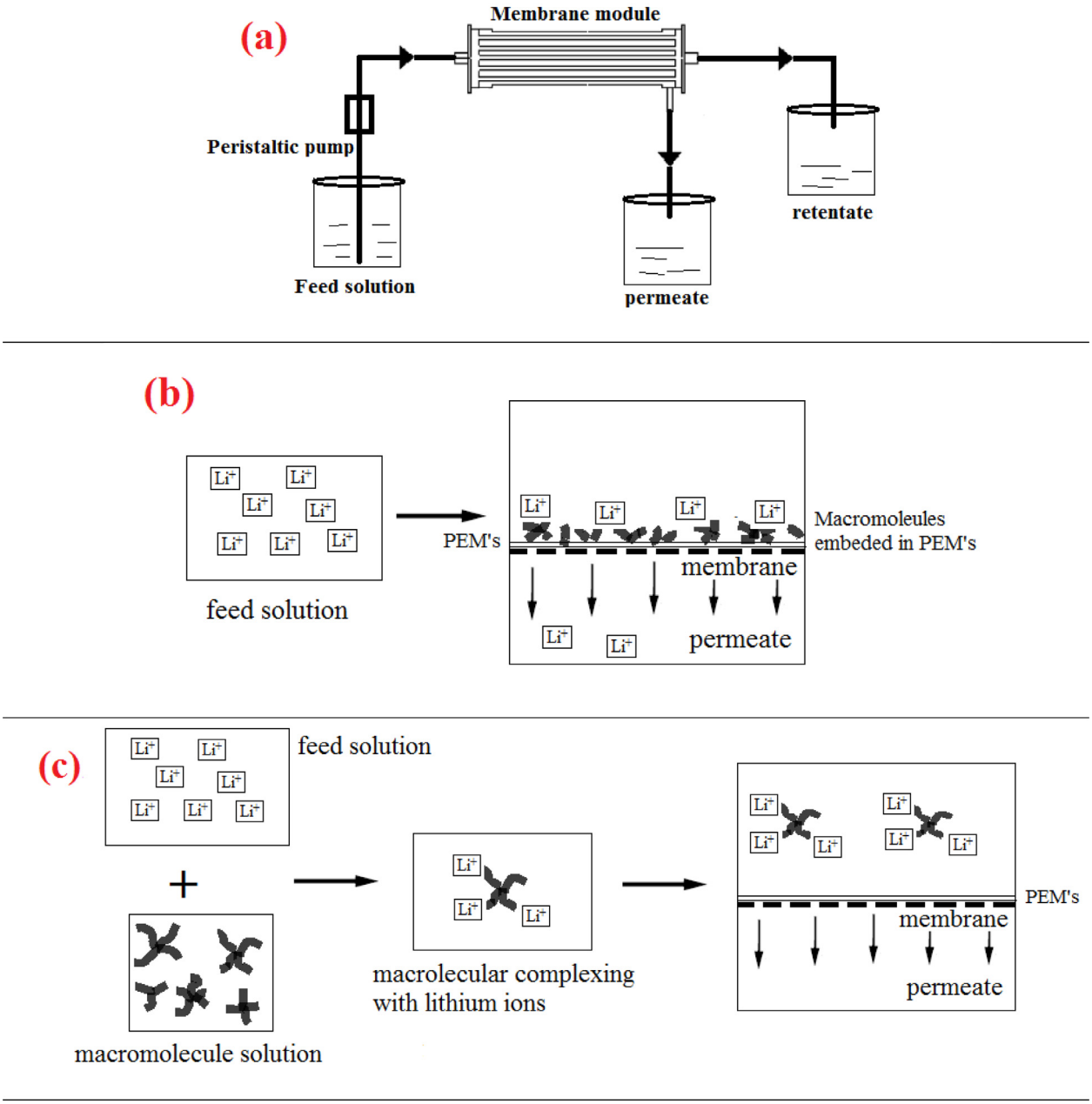

Fig. 1. Schematic representation of ultrafiltration setup (a); (b) – MIUF and (c) – MEUF.

bond or electrostatic or by the combination of different types. In order to improve separation, the macromolecules can be bound to lithium ions, thus enlarging the molecular dimensions of smaller ion components to be separated. The principle is to add an effective binding agent to metal ion solution so that this agent will complex with smaller sized metal ions which would easily pass through the PEM membranes during ultrafiltration.

2.4. Characterization of MIUF membranes and analysis method

The MIUF membranes were characterized by using UV–vis spectroscopy (Shimadzu 2450), ATR-FTIR (Shimadzu IR Prestige-21), SEM (JEOL JSM-6390), AFM (Veeco Nanoscope 3D, USA), spectroscopic ellipsometry (M − 2000 V, J. A. Woollam Co.) and contact angle meter (GBX Scientific Instruments, Ireland). The reliability of MIUF membranes was monitored via UV–vis and FTIR spectroscopy. The IR absorption spectra were recorded with an average of twenty scans per spectrum using an ATR attachment with a ZnSe crystal. The relative changes in the frequencies of the specific functional groups of TA and CHT in the PEM's were used for monitoring the modification. MIUF membrane morphology analyses were carried out with Scanning Electron Microscopy (SEM) and atomic force microscope (AFM). Average thickness measurements of MIUF and MEUF membranes were carried out by spectroscopic ellipsometry using an Inc M − 2000 V ellipsometer (J. A. WoollamCo.). Measurements were carried out in autonulling mode in PCSA configuration with 50–900 nm of spectral range. The ellipsometry thickness of MIUF and MEUF multilayer membranes was measured at incident angles of 65°, 70° and 75°, near the Brewster angle for the support material (silicon–SiO_2wafer) in order to obtain results with the highest possible sensitivity. All the

measurements were repeated at 5 different points on the sample and the spectra were analyzed using the B-spline model with Complete EASE v4.81 software. The thickness values were represented as mean ± standard deviation.

For the study of the hydrophilicity by measuring contact angle of the MIUF and MEUF membrane surfaces, GBX Scientific Instruments contact angle analyzer (Digidrop Contact Angle Meter used with Windrop software) was used. The instrument is equipped with a CCD camera, a sample stage and a syringe holder. Static contact angles of distilled water on modified membranes surfaces were measured by the sessile drop method at 25 ∘C and at about 65 % relative humidity. The volume of the water drops used was always 2 μL. All the lithium metal ion samples (Li^+ ions) were prepared at a concentration of 10^{-3} mol/L by further dilution from the stock standard solution of 1000 ppm. The concentration of metal ions in the feed and permeate were monitored by Dionex 1100 ion chromatography (IC). Ion chromatography, with an IonPac CS12 column and a conductivity detector, was used for the quantification of lithium ion. The eluent was methanesulphonic acid (MSA, 20 mmol/L) at a flow rate of 1.0 mL/min (Zeng et al., 2006). All the adsorption experiments were done in replicate. The relative deviations were in the range of ± 1.0%.

The rejection percentage (R %) was calculated by using the mathematical expression,

$$R\% = (1 - Cp/Cr) \times 100 \quad (1)$$

where R is the rejection in percentage, Cp and Cr are the concentrations of permeate and the retentate respectively (Chandra and Mohan, 2020).

The permeate solution flux, F, was calculated using Eq. (2), where V is the volume of permeate collected, A is the effective membrane area, and Δt is the sampling time (Baker, 2011).

$$F = V/A\Delta t \quad (2)$$

3. Results and discussion

3.1. Characterization of modified membranes

The PEM membrane in both MIUF and MEUF is just a barrier or a host that has to retain everything bound to TA and CHT, thereby restrict the passage of lithium ions. From this viewpoint, the membrane characterization is important in terms of macromolecules immobilized, surface morphology and thickness. Surely the surface properties of the PEM membrane material can influence the separation process, but the interaction between the macromolecules and metal ions is more significant. The MIUF membranes subjected to UV–visible spectroscopic analysis yields the following spectrums in Fig. 2(a) and (b). The electronic absorbance of 8 bilayer CHS/PSS PEM membranes with increasing concentrations of TA and CHT showed a linear increase with increasing concentrations of TA and CHT confirmed its appropriate presence in PEM's. A strong absorbance band was observed around 314 nm in case of TA immobilized membrane samples, while that for CHT immobilized membranes, the absorption peak is at 319 nm. The λ_{max} at 314 nm is due to the transition of a non-bonding (lone pair) electron on the oxygen atom of TA to a π* antibonding MO (n – π*) transition (Vinogradova et al., 2004). Thus sequential increase in both cases helped to concluded that TA and CHT were successfully incorporated uniformly into the coated membranes which may resulted the swelling of membranes.

The macromolecular development on the supporting PEM membrane is also clear from ATR-FTIR. Fig. 3(a) represents the FTIR spectra of 8 bilayer CHS/PSS PEM membranes with increasing concentration of TA, and the Fig. 3(b) is that of increasing concentration of CHT. In Fig. 3(a), the peak at 1486 cm^{-1} is due to aliphatic CH_2 and C-CH_3 bending vibrations and peak at 1580 cm^{-1} is due to aromatic stretching vibrations of C = C of TA. The increased intensity of these corresponding peaks with respect to the concentration of TA, suggested that TA has been successfully incorporated into the 8 bilayer PEM (Kavitha and Kandasubramanian, 2020; Kraal et al., 2006; Fu and Chen, 2019). From Fig. 3(b), the peak at 1106 cm^{-1} is due to C—C backbone stretching, 1151 cm^{-1} due to C—O stretching vibration and inplane C—H bending and 1242 cm^{-1} peak is caused by interaction of O—H bending and C—O stretching in C—O—H group of CHT as well as CH_2 deformations of CHT (Gupta et al., 2014; Palombo et al., 2009; Jaswal et al., 2015). The growth of these respective peaks of CHT indicates the proportionate immobilization of CHT among various PEM's.

The average dry thickness of the immobilized TA and CHT were determined by ellipsometry method. The average thickness calculated from the values obtained from three measurements at five points on substrate. The results obtained from approximation are presented in Fig. 4. The PEM's without TA and CHT are used as a reference and to compare the increase in thickness with immobilization. It is clearly shown that the macromolecular adsorption on PEM has a huge impact on membrane system with a hike in membrane thickness. The results show that as more macromolecules get deposited, the average thickness also got uniformly increased with an increasing grain size.

The data obtained from Fig. 4 is in comparison with the trend that has been observed in the spectroscopic analysis. The plot between thickness and amount of macromolecular immobilization in MIUF membranes showed a linear incorporation of macromolecules into the PEMs. This increase in thickness of PEM membranes might be due to the swelling of PEM after the increased deposition of TA and CHT. The better binding capacity of TA macromolecules due to its higher number of binding sites and macromolecular nature results a steady linear growth in thickness. In the case of CHT with a complex ring structure, this was not so favourable as compared with TA for complexing in between the PEM's (Goossens et al., 2008). As a result of this macromolecular behaviour, MIUF with TA is exhibiting a much thicker PEM complex than CHT based MIUF membranes. This difference in immobilization pattern can be attributed to its nature itself. The difference in pattern between two phases (before and after immobilization) might be due to the in and out diffusion nature of higher concentration of CHT molecules in nano bilayers (Metzler et al., 2016).

The bilayered and MIUF membranes were subjected to AFM analysis (Fig. 5) which revealed an extreme rough and highly porous morphology due to its fabrication and deposition. It should be noted that for PEM membranes containing macromolecule, the surface roughness mainly depends on the outermost layer as well as the macromolecule. The roughness was significantly increased, when an additional macromolecule was deposited atop. Image J software was used for pore size approximation from AFM images. The pore size values of PEM (8 bilayer) and that with high TA concentration were found to be 0.118 ± 0.33 nm, and 0.23 ± 0.41 nm respectively. The average pore size value calculated for PEM with higher CHT deposition was found to be 0.92 ± 0.62 nm. The average RMS roughness values were approximated using Gwyddion software. The values obtained for PEM, PEM with high TA deposition and PEM with higher CHT depositions were 234.43 nm, 395.43 nm, and 306.52 nm respectively. The CHT based MIUF membrane had found have lower roughness when compared with TA based MIUF membranes. The complexity in the nature of CHT played a big role in the lower surface roughness of CHT based MIUF membrane. The inherent hydrophobic nature of CHT always hinders its immobilization into bilayers with lesser roughness and thickness (Bou Saab et al., 2013). Also, the possible hydrophobic repulsion between immobilized CHT and the PSS anionic layer of PEM facilitates the same trend (Tan et al., 2005).

The formation of MIUF PEM has been examined and confirmed using SEM. SEM images of PEM (8 bilayer) membrane, MIUF (TA) and MIUF (CHT) PEM membranes were presented in Fig. 6. SEM images of all membranes were found to be highly rough, while all showed good porosity expect for TA immobilized (Fig. 6(b)). The porous PEM surface has transformed into a uniform, thick, aggregated and

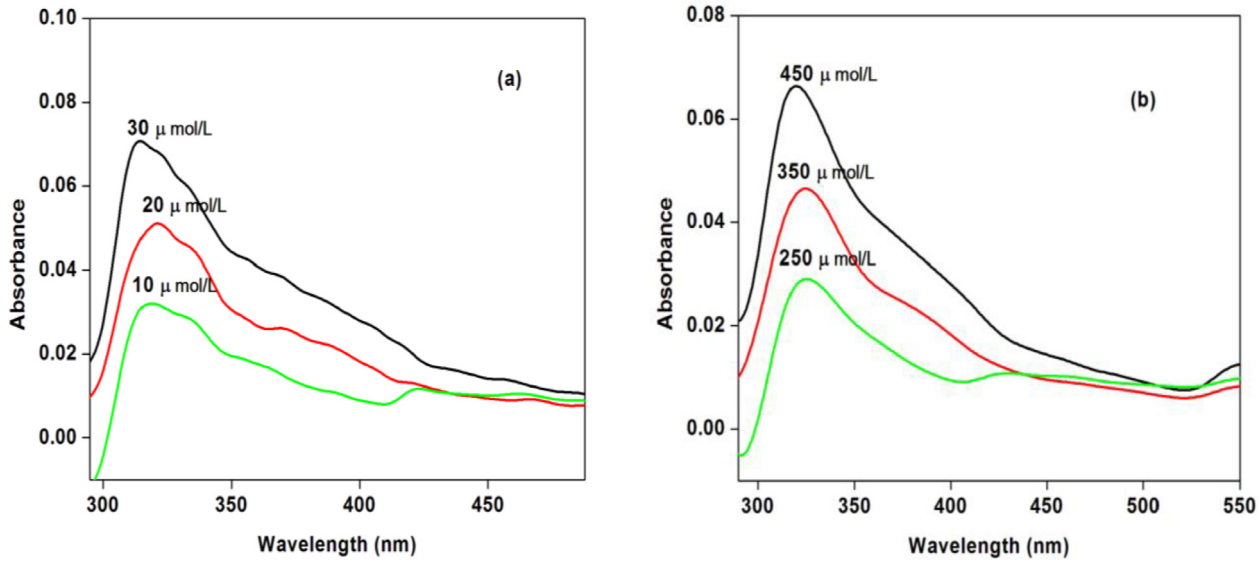

Fig. 2. UV–vis spectra of MIUF membranes (8 bilayer) ((a) – TA and (b) – CHT).

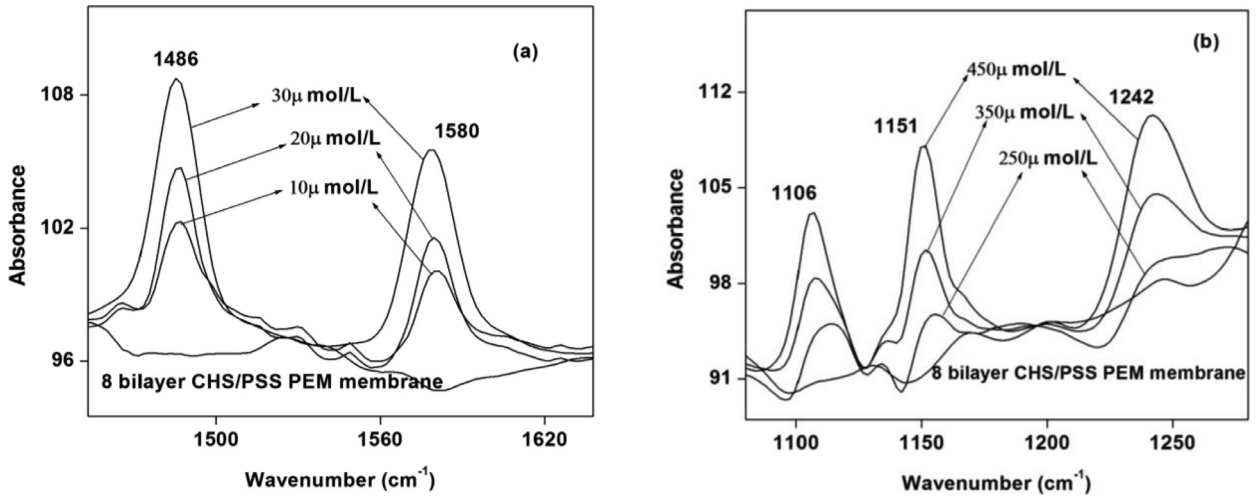

Fig. 3. ATR-FTIR absorption spectra of MIUF membranes (8 bilayer) ((a) – TA and (b) – CHT).

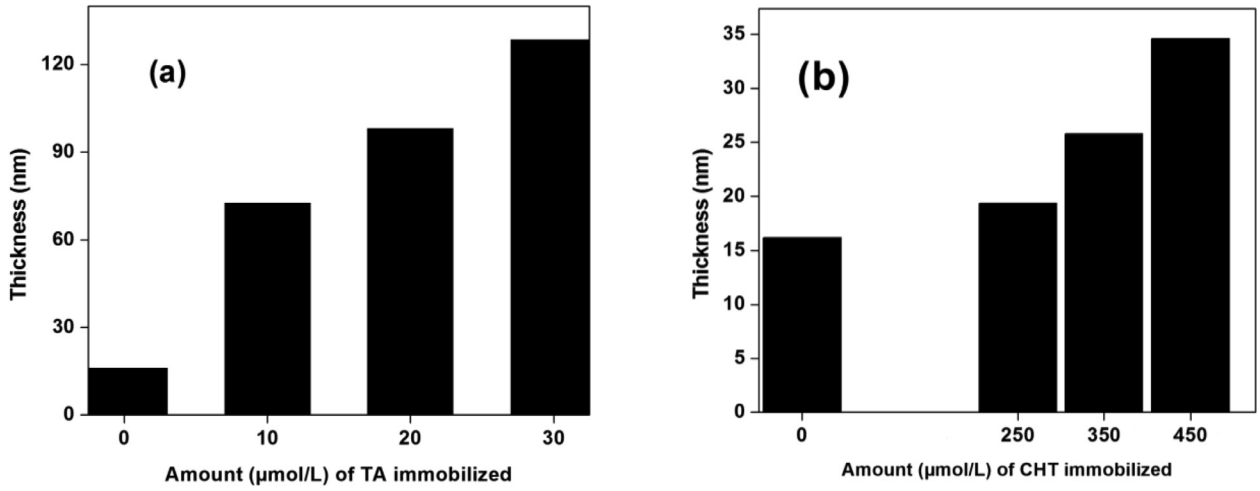

Fig. 4. a) Average thickness of MIUF with TA b) Average thickness of MIUF with CHT.

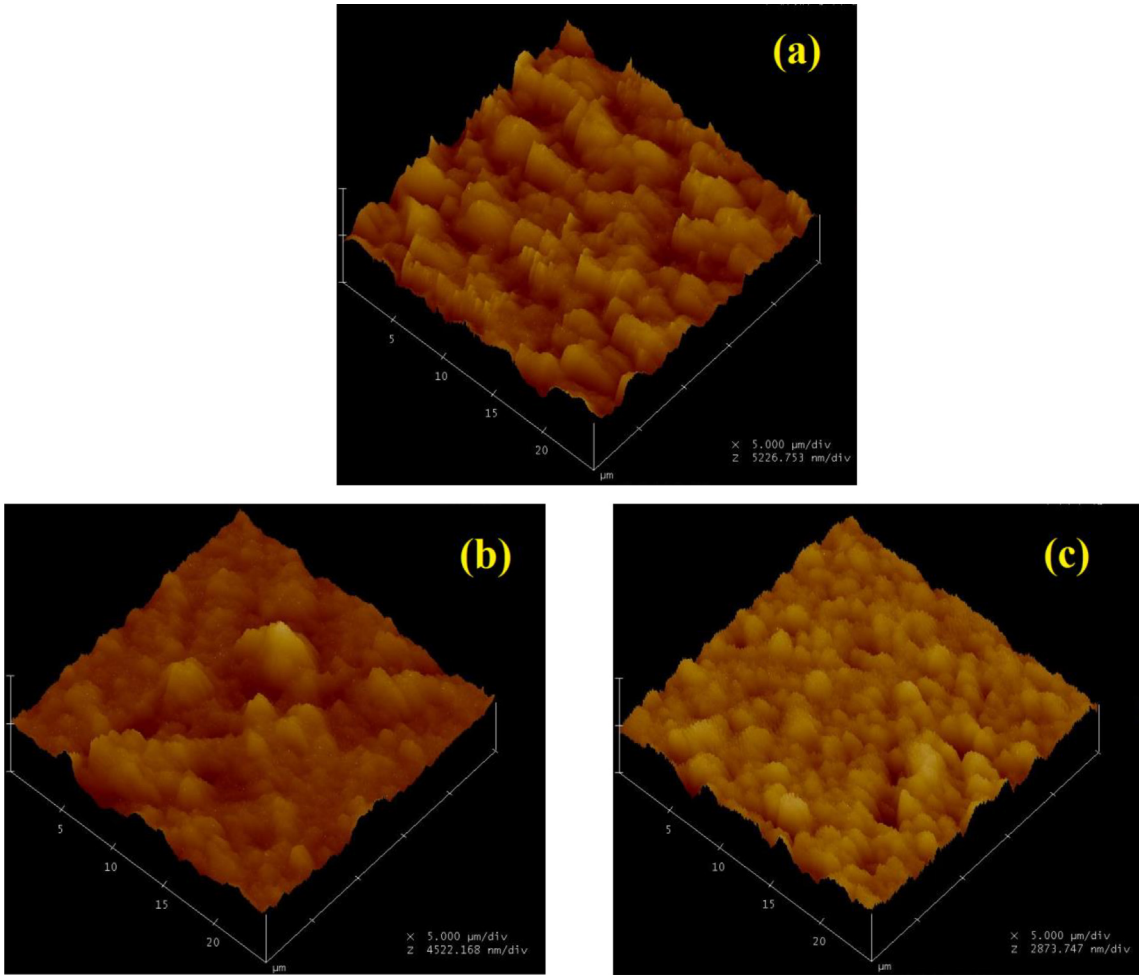

Fig. 5. AFM images (3D) of 8 bilayer MIUF membranes ((a) – normal PEM, (b) - TA (30 μmol/L), (c) - CHT (450 μmol/L).

fully covered morphology after TA immobilization. The CHT immobilized membrane surface showed significant morphological difference with TA immobilized PEM membranes, with poor pore coverage for the former. The difference in morphologies of MIUF PEM is a clear indicator of effective fabrication by immobilization. The PEM membrane surface roughness was also found to increase with immobilization and also with increased macromolecule concentration over PEM surface.

The immobilization of any macromolecule can cause the surface pore blockage and can sometimes limit the membrane permeation properties unless otherwise they are highly hydrophilic in nature. In order to examine the hydrophilicity, the immobilized nano PEM membranes were examined by contact angle measurement. Fig. 7 shows the hydrophilic nature of modified membranes with an average water angle contact of 25.5° and 36.1° for TA and CHT respectively. These readings indicate that the exposed substrate is fairly hydrophilic, which increases water permeation and hence, water flux. The wettability of the membrane changes with modifications as the chemical composition of the exposed layer, the hydrophilicity of its functional groups, and the level of immobilization which can influence its permeation behaviour.

3.2. Effect of macromolecule immobilization on PEM membrane flux

The variation of macromolecule immobilizing flux as a function of the number of bilayers for different concentration of TA and CHT were shown in Fig. 8(a) and (b) respectively. In the case of TA and CHT, it was found that the immobilization flux decreases with an increase in number of nano bilayers. Also, they showed similarity in immobilization flux when there is an increase in nano PEM macromolecular concentration. The decrease in flux can be assigned to the increased macromolecular concentration in nano PEM and due to the increased number of bilayers. This caused an additional surface coverage and correspondingly more number of pores gets closed. The higher flux for CHT immobilized nano PEM membranes was due to the hydrophobic nature of CHT than TA.

3.3. Ultrafiltration studies of MIUF PEM membranes

3.3.1. Effect of number of bilayers and concentration of macromolecules

The spiked metal ion aqueous solution at concentration of 10^{-3} - $molL^{-1}$ was ultrafiltered through TA and CHT based MIUF PEM membranes. As discussed earlier, PEM membranes comprising of weak CHS and strong PSS polyionic combination ranging from 2 to 8 bilayers were used in all experiments. The performance of bare and MIUF PEM membranes was experimented for the lithium ions with respect to different permeation characteristics. The percentage rejection values and flux against the number of functional layers under two filtration modes are shown in Figs. 9 and 10.

The highest percentage rejection attained by MIUF membranes is ~ 84.13 %, where the bare membrane showed a low rejection efficiency of ~ 25.34 % only. In both types of MIUF membranes (TA and CHT), the rejection efficiency increases with increase in number of bilayers with a linear rejection pattern. The results showed that

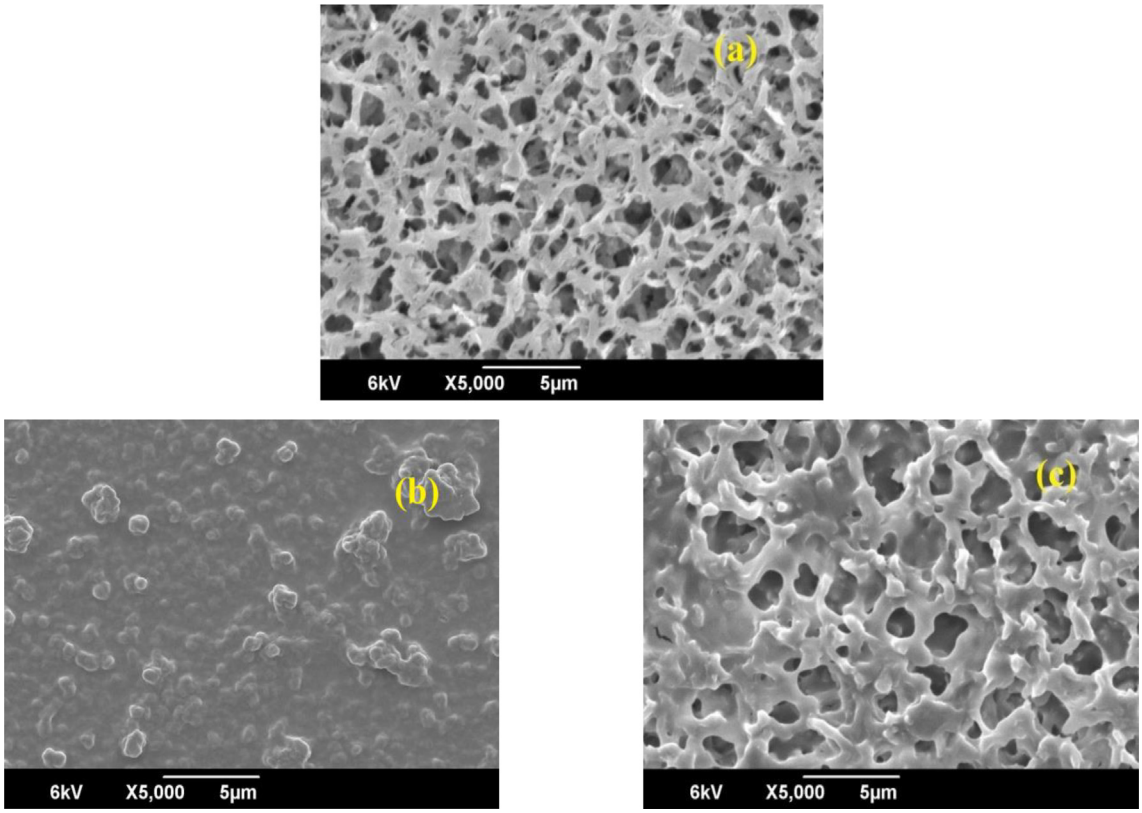

Fig. 6. SEM images of PEM membranes (8 bilayer) ((a) normal PEM (b) TA (30 μmol/L), (c) - CHT (450 μmol/L)).

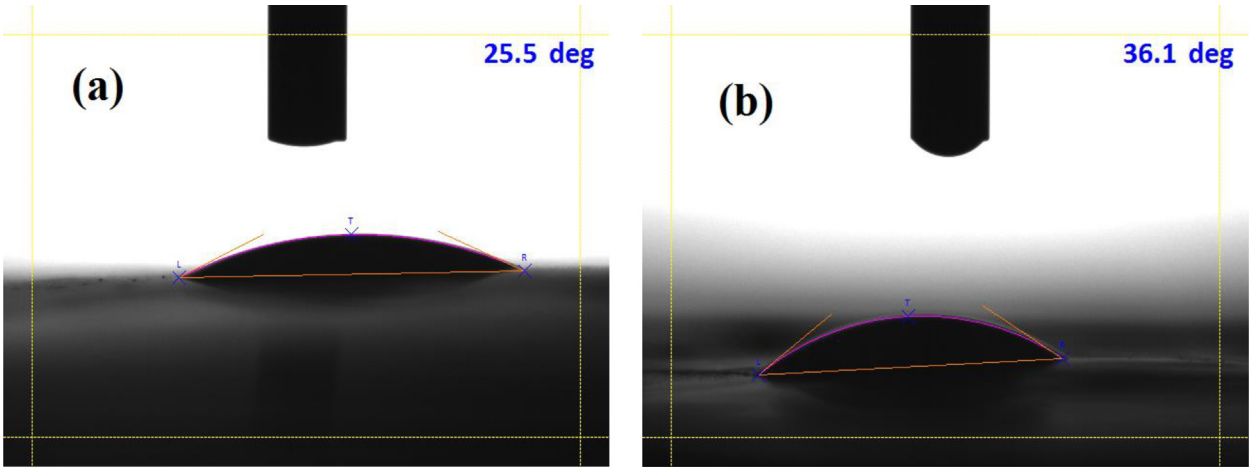

Fig. 7. Contact angle measurement of PEM (8 bilayer) at 20 s ((a) TA (30 μmol/L), (b) – CHT (450 μmol/L)).

the rejection efficiency of this filtration mode depends mainly on the macromolecule concentration immobilized between the PEM's. The rejection also showed a positive trend with increased roughness values from AFM images (Fig. 5) due to increased surface area by immobilizing macromolecules. Fig. 9(a) and (b) displayed the variation of lithium retention as a function of macromolecule concentration. It shows that when macromolecular concentration increases in MIUF membranes, lithium ion retention also got increased until reaching highest retention rate of ~ 82.51 % and ~ 84.13 % respectively for high concentration of TA and CHT.

The possible factor that fosters the rejection by bare membrane (~25.34%) could be the membrane surface charge. Even though ultipore holds some amphoteric nature, the inherent overlapping cationic surface nature enabled the bare membrane to repel the like charges in an effective manner. This has influenced the lithium rejection with bare ultipore with an efficiency of about 40 % in the filtration experiments being done at pH ranging between 6 and 6.5. This filtration condition (isoelectric point of ultipore is 6.3) had enhanced the electrostatic repulsion between the lithium ions and membrane charged sites, contributing to the better sieving mechanism. The immobilized concentration of macromolecules along with the increased number of CHS/PSS bilayers also played an important role for good rejection efficiency (Sylwia et al., 2019).

From Fig. 9(a) and (b), it can be clearly seen that the rejection efficiency has increased as the number of bilayers increased from 2 to 8. For PEM's without macromolecules, the rejection efficiencies were

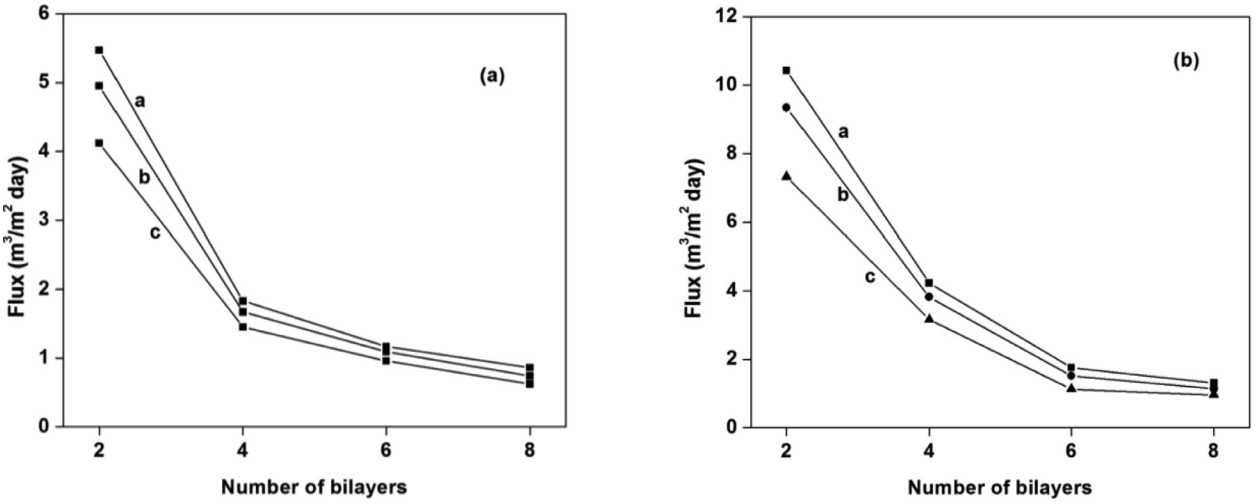

Fig. 8. The immobilizing flux of various PEM membranes with macromolecular immobilization [a) TA and b) CHT]

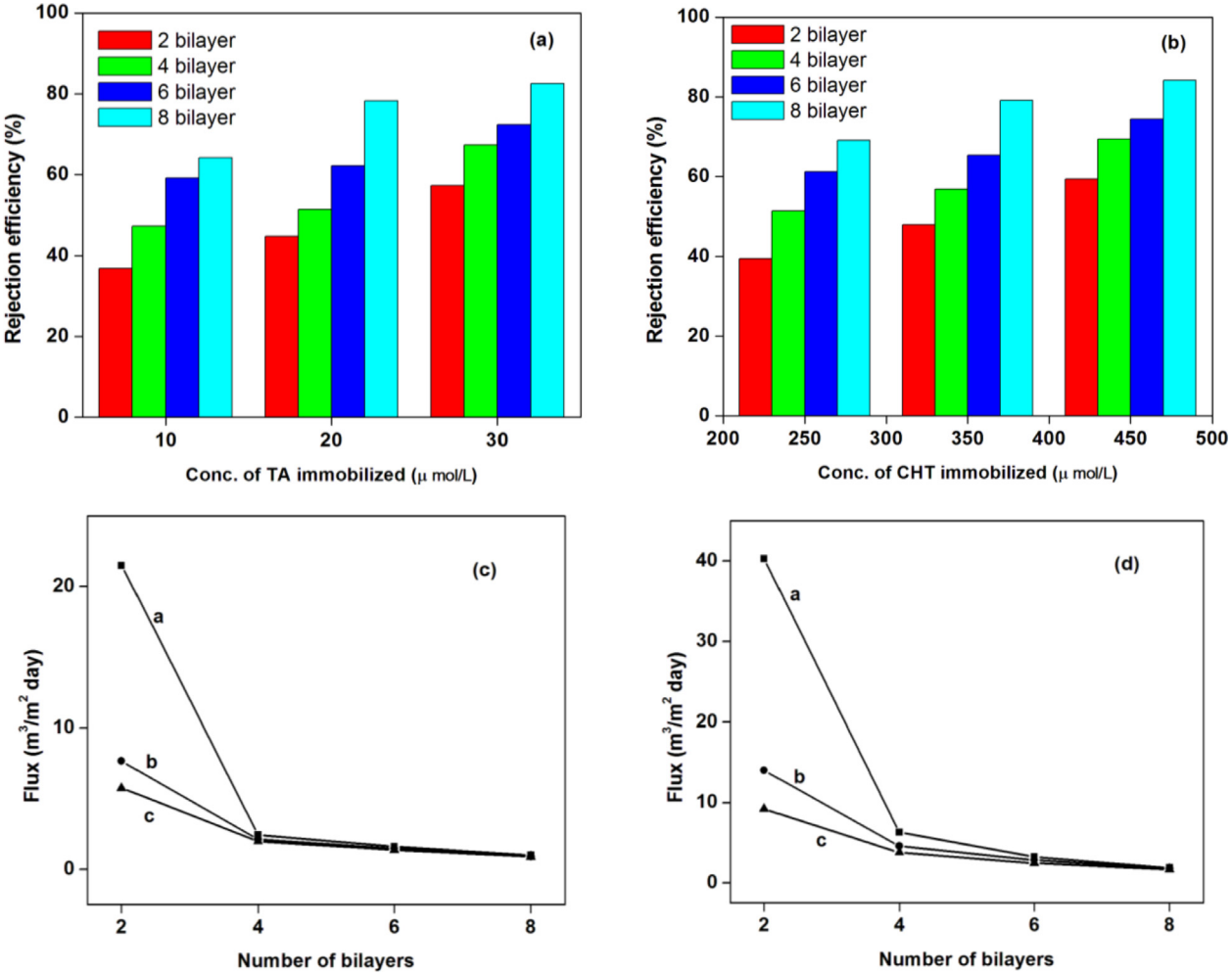

Fig. 9. Rejection efficiency and permeate flux of MIUF PEM membranes [a) & c) - TA, b) & d) - CHT]

27.52, 32.41, 40.84 and 44.52 % for 2, 4, 6 and 8 bilayer PEM membranes respectively. For lower concentration of TA, the rejection efficiencies were 36.87, 47.2, 59.12 and 64.21 % for 2, 4, 6 and 8 bilayer PEM membranes respectively. This rejection efficiency has been increased when the PEM membrane system was fabricated with higher concentration of immobilization within the MIUF membranes. The rejection efficiencies achieved in the case of medium concentration of TA in MIUF membranes were 44.84, 51.34, 62.18 and 78.21 % for 2, 4, 6 and 8 bilayer PEM systems respectively. The efficiency has further improved with high TA immobilization which showed a

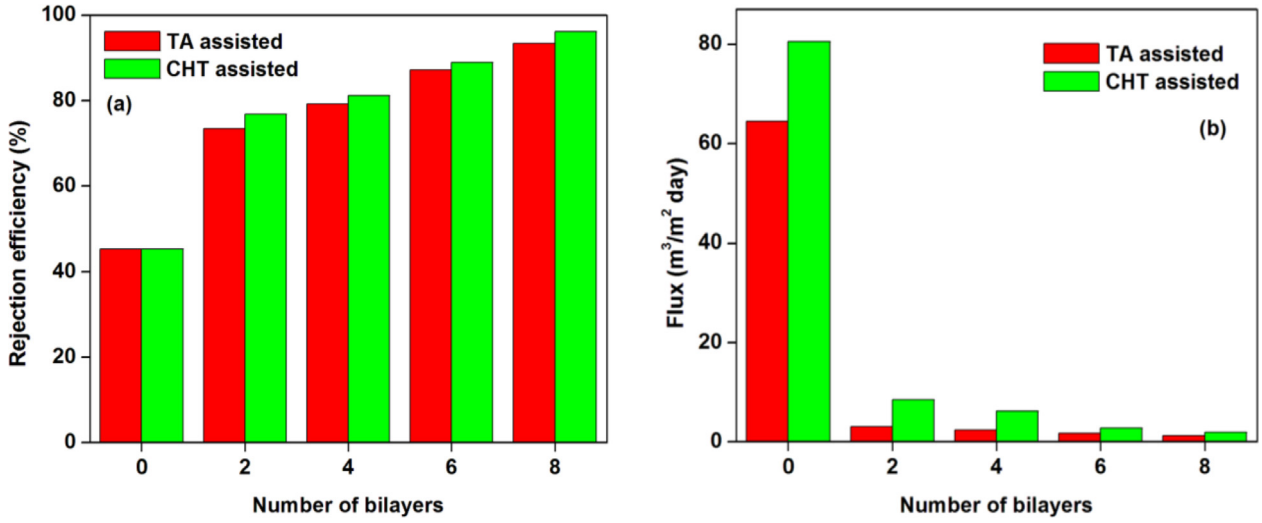

Fig. 10. Rejection efficiency and permeate flux of MEUF PEM membrane filtration for Li^+ ions, a) rejection efficiency b) permeate flux.

rejection of 57.3, 67.28, 72.38 and 82.51 % for 2, 4, 6 and 8 bilayer PEM membranes respectively.

The rejection efficiency of CHT based MIUF PEM membranes was found to be better than the TA based MIUF PEM membranes. The rejection of lithium ions by TA based MIUF PEM membranes is expected by the interaction of anionic PSS layer of PEM with metal ions and also by the complexation of metal ions with carboxylic groups in tannic acid (Wang et al., 2020). In case of CHT based MIUF membranes, the interaction between the metal ions and CHT molecules leads to the formation of chelating complex (Dong et al., 2019). It has already reported that benzimidazole gets attached to hydrophobic part of sterols for metal ion chelation (Zhang et al., 2014). The high rejection efficiency of CHT based MIUF membranes than the other with TA might be attributed to highly porous morphology and strong dipole-ion interactions between metal ions with carboxylic acid groups of CHT. The recovery efficiencies attained with low concentration of CHT immobilization achieved about 39.47, 51.39, 61.23 and 69.12 % for 2, 4, 6 and 8 bilayer PEM membrane systems respectively. The rejection efficiencies achieved in case of medium concentration of CHT were 47.85, 56.85, 65.39 and 79.12 % for 2, 4, 6 and 8 bilayer PEM membrane systems respectively. Finally, the efficiency attained 59.34, 69.34, 74.39 and 84.13 % for 2, 4, 6 and 8 bilayer PEM membrane systems respectively with high concentration of CHT immobilization. Thus, it is concluded that the CHT based MIUF PEM membranes were found to be slightly better than the TA based MIUF PEM membranes for effective removal of Li^+ ions from water. Anyway, the optimal number of bilayer is surely eight with CHT immobilized within it possessing about ~ 84 % rejection efficiency.

Permeate flux was calculated by keeping the applied pressure and feed volume of lithium ion solution intact and the curve was plotted with flux (m^3/m^2 day) versus number of bilayers. Fig. 9(c) and (d) represents the variation of permeate flux as a function of number of CHS/PSS bilayers with different concentration of macromolecules immobilized within PEM membranes. In both cases, the permeate flux decreases with increase in feed macromolecule concentration (a > b > c). (a- low concentration, b- medium concentration and c- high concentration of macromolecules) The increased macromolecule concentration over PEM membranes increases the solution viscosity and density (Reddad et al., 2002). Also, the higher macromolecule concentration tends to depromote the turbulence and causes higher concentration polarization, resulted a lower flux of nano PEM membranes (Hu et al., 2006). Thus, the decrease in permeate flux with increase in number of bilayers can be attributed to the increase in concentration of polyelectrolytes as well as macromolecules in PEM's.

In MEUF experiments, the macromolecules (TA and CHT) were dissolved in the spiked metal ion solutions and allowed to attain equilibrium. The metal ions-macromolecule complex is then ultrafiltered with bare membrane and PEM membranes. A comparison of TA and CHT based MEUF is depicted in Fig. 10(a) with permeate flux (10 (b). From the Fig. 10, it is clear that CHT based MEUF was found to be more efficient than TA based filtration. The change in chemical interaction ability of TA and CHT with metal ions might possibly the reason behind the difference in efficiency of MEUF. The theory of MEUF involves the effective binding of metal ion with macromolecule to form chelating complex, followed by its effective steric blockage by PEM's. Different studies showed that the chelating complexes were better rejected by PEM membranes (Huang et al., 2009). The rejection efficiency by this mode attained efficiency above 60 % even with 2 bilayered PEM. The recovery efficiency for TA and CHT based MEUF membrane systems were 93.42 % and 96.11 % respectively, whereas the recovery efficiency without macromolecular assisted attained only about 45.34 %. Thus, it can be conclusively confirmed that the macromolecules has complexed effectively with the metal ions forming a chelating complex which can be efficiently rejected by PEM.

Bare membrane flux with MEUF membrane fluxes of TA and CHT were shown in Fig. 10(b). When the transmembrane pressure was kept constant, the metal permeation flux and the secondary resistance of macromolecules were dependent on the macromolecule concentration and their molar ratio. The macromolecule-ion complexation caused an increase in viscosity of stock solution causing a decrease in mass transfer coefficients results a decline in permeate flux across PEM membranes. The macromolecules deposited on bilayer surface during filtration generate an additional resistance against the solvent transmembrane flux. Additionally, the concentration polarization was caused by the accumulation of retained solutes (Rivas and Moreno-Villoslada, 1998) resulting a decreased flux. As the concentration polarization was not severe, the decline in permeate flux was comparatively low with MIUF method.

3.4. Comparison of MIUF and MEUF PEM filtration modes

When comparing MIUF and MEUF modes, MEUF mode is found to be more efficient than the latter in terms of efficiency and simplicity. Again, if the comparison is made in terms of macromolecules used either in MIUF or MEUF, the CHT used mode is found to be more efficient than TA. The important factor that governs rejection of lithium ions is electrostatic interaction rather than its steric factor. In MIUF mode, the macromolecules immobilized helped to increase the binding

sites to many folds along with PEM sites, which should enhance the metal ion--PEM membrane interactions. The charged polyelectrolytes have the capacity to interact with solute particles (Sablani et al., 2001). Due to smaller size of metal ion solutes, PEM alone fabricated over membranes were not able to resist its permeability. The presence of large molecules like tannic acid and campesterol converted the ordinary PEM membrane into more active and efficient system for metal ion rejection. The easiness in metal ion macromolecular interaction and less complexity helped to deliver an excellent rejection results for macromolecular assisted ultrafiltration mode than the other. The mechanism involves for this type of metal ion-macromolecule is better explained and elaborate with normal types of aggregate formation theory or by simple adsorption mechanism or by coagulate formation mechanisms (Qdais and Moussa, 2004).

The results indicated that the performance of both TA and CHT based MEUF PEM membrane systems for lithium ions attained good rejection of about 93.42 % and 96.11 % respectively. When MEUF PEM membranes were compared with other membranes based rejection experiments, it showed sound superiority over these methods. For example, Wen X. et al. (2006) reported the recovery of lithium by nanofiltration Desal-5 DL membrane with only 55% efficiency. Similarly, another study by Chung K et al. (2008) used an inorganic adsorbent containing polymeric membrane reservoir for the recovery of lithium with about ≤ 90% rejection. A study conducted by Samuel B. et al. (2017) showed the ability of bipolar membrane electrodialysis (BMED) for simultaneous separation and recovery of boron and lithium from aqueous solutions. Here also, the method could only reach an efficiency of about ≤ 90% for lithium ions. Wenhui S. et al. (2019) fabricated a membrane capacitive deionization module for the removal of Li^+ which reached only about 38.4 %. Another study by Mohammad K. et al. (2020) utilized crown ether containing polyelectrolyte multilayer membranes for lithium recovery and attained a recovery of 71.6% only. Recent studies by Ounissi T. et al. (2021) obtained a recovery rate that reached only 22.1% for lithium by diffusion processes using lithium composite membranes. Another recent study by Yakubu A.J. et al. (2021) demonstrated electrodialysis stacks having different ion exchange and bipolar membranes for simultaneous separation of boron and lithium from aqueous solution for which 86.4% was achieved for lithium. In summary, although there are many published reports on membrane based separation processes for lithium recovery, the MEUF technology holds with significant potential for further development and process scale up in the future.

3.5. Effect of solution pH

Solution pH is an important factor in water treatment sorption processes because it can influence the behaviour of polyelectrolytes (usually weak) and immobilized macromolecules and H^+ or OH^- act as competing ions in the filtration process. The effect of initial solution pH values (1–6) on Li^+ ion sorption onto PEM membranes using two filtration modes were investigated, and the results were shown in Fig. 11. From the results, it is clear that Li^+ removal was unfavorable in acidic media (pH ≤ 1), but rejection efficiency got increased with increasing pH value. There was only 58.49 % (TA in MIUF) and 63.56 % (CHT in MIUF) removal found at pH 1 that increased to 82.51 % and 84.13 % at pH 6 respectively. An improved rejection of 74.55 % (TA in MEUF) and 78.43 % (CHT in MEUF) was observed at pH 1 which got improved to 93.42 % and 96.11 % respectively at pH 6. But at low pH, the availability of H^+ ions in the solution is high and a possibility of competition between Li^+ ions with H^+ ions for interactive sites arise within the solution. As a result, a dip in metal ion-macromolecule occurs and chances of easy diffusion through the MIUF PEM membrane results with low rejection. As the pH increases the availability of H^+ ions decreases which results in an increased rejection. The same mechanism is applicable to assisted filtration mode also. At lower pH 1, the extent of ionization of the functional

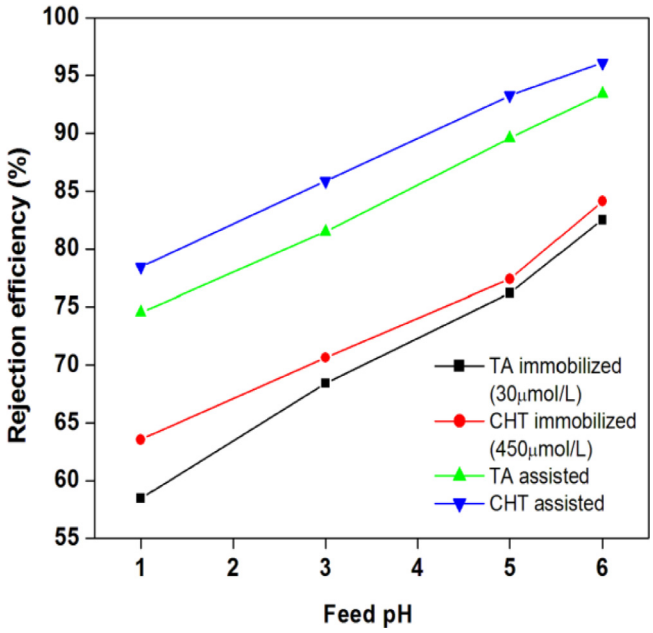

Fig. 11. Effect of feed solution pH on Li^+ ion removal.

groups present in PEM and macromolecules varies and hence the degree of multilayer cross links. This can affect the permeability and flux of the multilayer membrane. As the PSS is more ionized at pH 2.1, the resulting films at low feed pH can be consequently thinner (Ilyas et al., 2017; Petelska and Figaszewski, 2000). This morphological change can influence the immobilization or assisted filtration and consequently the removal efficiency of Li^+ metal ions.

3.6. Effect of added salt on the removal of lithium ions

The rejection efficiency of MIUF and MEUF PEM membranes in the presence of varying ionic strength (0–1 M of NaCl) were studied. Fig. 12 shows the effects of added salt concentrations on rejection values. The increase of salt concentration in feed leads to the compression of double electrical layer causing screening effect, and thus to the reduction of electrostatic attraction between lithium ions and interac-

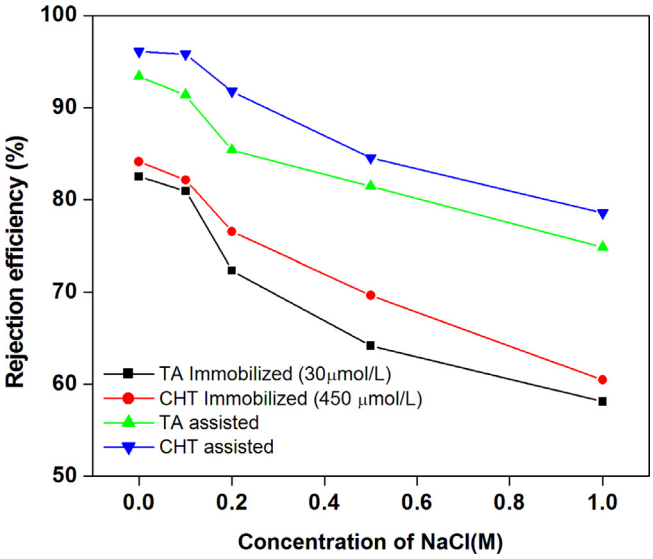

Fig. 12. Effect of salt concentration on Li^+ ion removal.

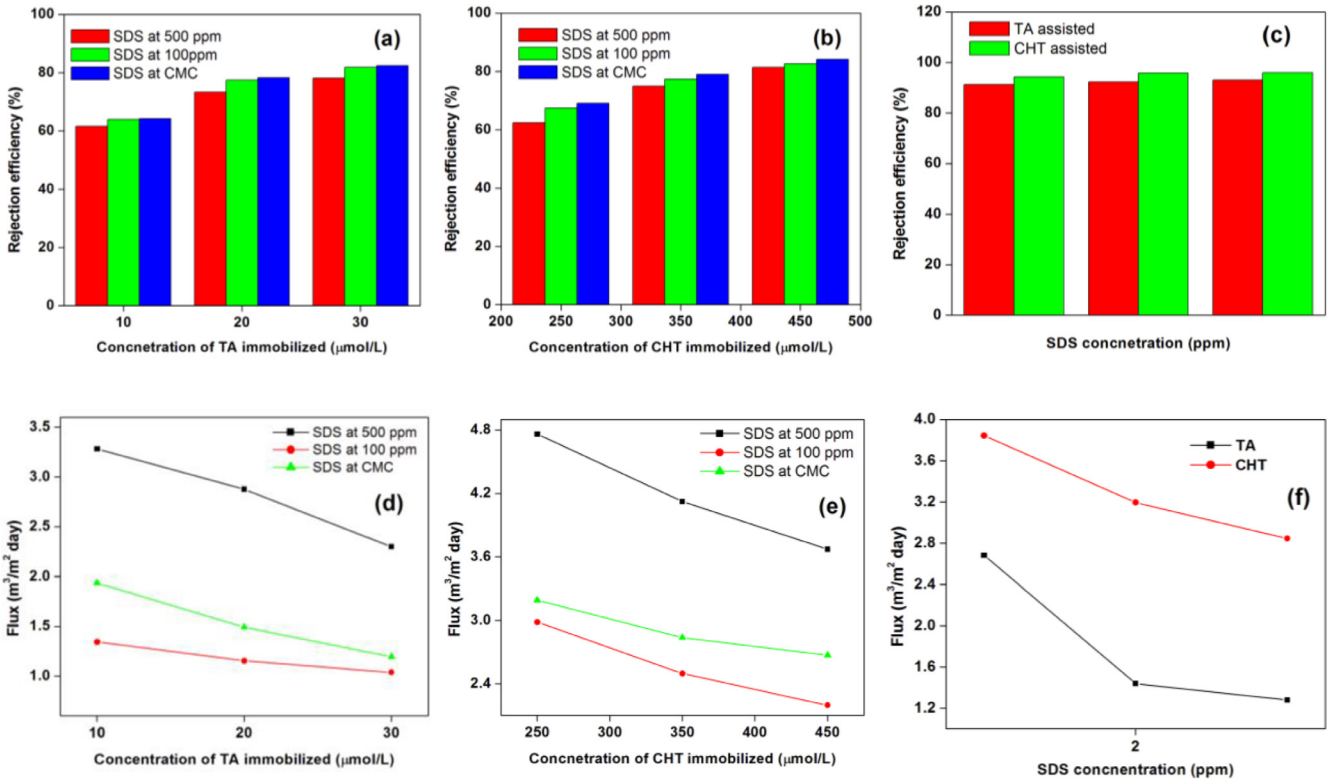

Fig. 13. Rejection performance and permeate flux of CHS/PSS 8 bilayer nano PEM membranes functionalized with macromolecules at different SDS concentration [a) & d) TA, b) &e) CHT, c) & f) Assisted mode]

tive sites (Zeng et al., 2009). As a result, the added salts can affect the retention of lithium ions. The presence of salt in feed also increases the surface roughness as well as pore size of MIUF and MEUF PEM membranes. Thus, screening effect of salt affect the interaction between charged membrane surface and the metal ions result a decrease in rejection of lithium ions.

3.7. Effect of surfactant

Sodium dodecyl sulfate (SDS) is a commonly found pollutant with anionic nature discharged into the environment degrading the water quality to a great extend. In order to study the rejection of lithium ions by two filtration modes in the presence of commonly found SDS, different concentration of SDS were used. The solubility of SDS varies with its concentration, usually increases at a concentration above its critical micellar concentration (CMC), 8.1 mM. The rejection of lithium ions with flux at different SDS concentration under two filtration modes is shown in Fig. 13.The performance of MIUF and MEUF modes at higher concentrations of SDS in the feed (500 ppm), at low concentration (100 ppm) and at CMC were evaluated.

The results from above Fig. 13(a–c) revealed that in the presence of SDS, the efficiency of the both MOUF and MEUF modes using PEM membranes had reduced to some extent. The extend of rejection was larger for rejections at higher concentration of SDS than the other two concentrations. The trend in rejection efficiency and flux of two filtration modes in the presence of SDS followed a similar way as in the absence of SDS. But, the rejection efficiency of two filtration modes decreased slightly while the permeation flux increased drastically in

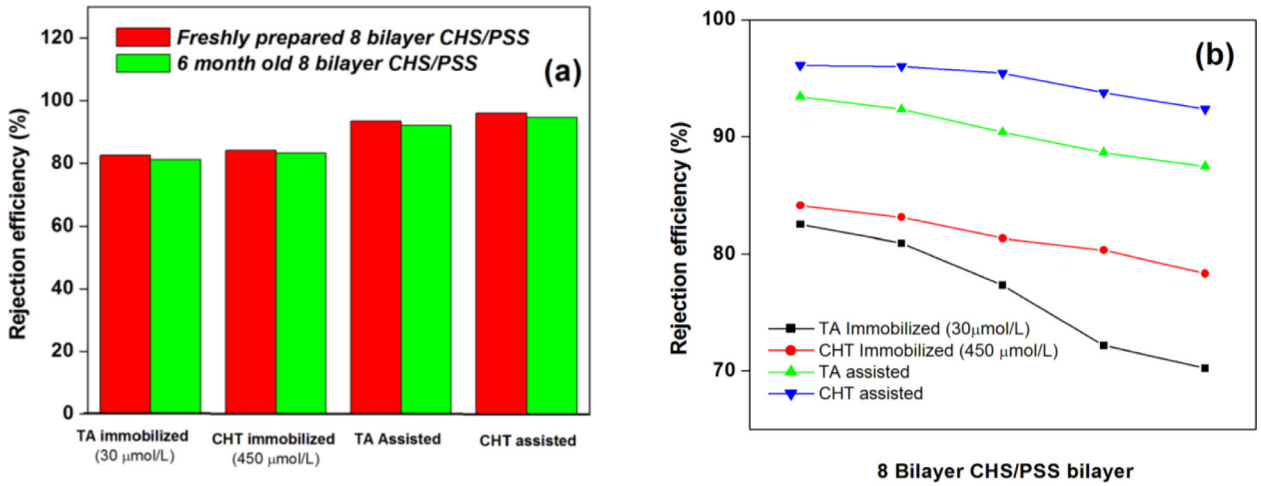

Fig. 14. Performance comparison of MIUF PEM (8 bilayer) membranes.

the presence of SDS. The comparison of permeate flux of MIUF PEM (8 bilayer) membranes in Fig. 13(d–f) showed that as the concentration of SDS increases, the flux also increased up to CMC and then falls. This increase in flux results from the decrease in the hydrodynamic resistance of the modified membranes in the presence of SDS. A linear relationship between the flux and concentration of SDS (below CMC) can be explained by application of the polarization model (Nikhil and Mothi, 2020; Wu et al., 2020). At pH > 5, the solubility of TA should be increased, therefore the TA particles stepwise will attain spherical structure, where the surfactant molecules may form the aggregates with hydrophobic interior of bulky TA micelles (Üçer et al., 2005), which can affect the binding efficiency of macromolecules resulted in a slight decrease in rejection efficiency. The decrease in metal ion transport rates which occur above CMC concentration was due to the covering of bilayer pores with SDS micelles by screening effect or mechanical blocking of pores by the surfactant.

3.8. Self life and reusability

In order to understand shelf life and reusability of MIUF PEM membranes, six months old and used MIUF membranes were experimented for the filtration of metal spiked water samples. The rejection of these older MIUF membranes showed a slight decrease in its efficiency than the freshly prepared ones (Fig. 14(a)). The reusability was also tested by repeating filtration five times with same membranes (Fig. 14(b)). The decrease in efficiency in repeated filtration might be due to the decrease in its interactive sites which permits an easy permeation of metal ions through it when compared to fresh PEM membranes.

4. Conclusion

The consumption of energy storage metal lithium is increasing day by day and estimated to grow exponentially. Hence to favor a clean environment and to support environmental regulation and lithium metal economy, it is also essential to recover the metals from secondary sources. In this study, a green process with prospective environmental and economic significance has been experimentally established for the sustainable recovery and removal of lithium ions from water. Two membrane based systems (MIUF and MEUF modes) were explored for the application of lithium recovery. According to rejection results, the MIUF PEM membranes (both TA and CHT) reveal almost similar and sound rejection abilities (~>80%), while the MEUF PEM membranes with TA and CHT metal ion complexation showed superior rejection performance (~94% and ~96%) under the optimized conditions. The feed pH is an important factor which can influence the lithium ion rejection. An optimum pH of 6 showed highest rejection when compared with lower feed pH. Compared with conventional electrolysis and causticization reaction process, macromolecule assisted method provides an environmental friendly and cost effective process for removal of lithium ions from water.

Declaration of Competing Interest

The authors declare that they have no known competing financial interests or personal relationships that could have appeared to influence the work reported in this paper.

References

Xu, P., Hong, J., Qian, X., Xu, Z., Xia, H., Tao, X., Xu, Z., Ni, Q.-Q., 2021. Materials for lithium recovery from salt lake brine. J. Mater. Sci. 56 (1), 16–63. https://doi.org/10.1007/s10853-020-05019-1.

Battistel, A., Palagonia, M.S., Brogioli, D., La Mantia, F., Trócoli, R., 2020. Electrochemical methods for lithium recovery: a comprehensive and critical review. Adv. Mater. 32 (23), 1905440. https://doi.org/10.1002/adma.v32.2310.1002/adma.201905440.

U.S. Geological Survey (2020). Mineral Commodity Sum-maries 2020. U.S. Geological Survey, Reston. https://www.usgs.gov/centers/nmic/mineral-commodity-summaries.

Lv, W., Wang, Z., Zheng, X., Cao, H., He, M., Zhang, Y.i., Yu, H., Sun, Z., 2020. Selective recovery of lithium from spent lithium-ion batteries by coupling advanced oxidation processes and chemical leaching processes. ACS Sustain. Chem. Eng. 8 (13), 5165–5174. https://doi.org/10.1021/acssuschemeng.9b0751510.1021/acssuschemeng.9b07515.s001.

Chen, X., Luo, C., Zhang, J., Kong, J., Zhou, T., 2015. Sustainable recovery of metals from spent lithium-ion batteries: A green process. ACS Sust. Chem. Eng.. https://doi.org/10.1021/acssuschemeng.5b01000.

Ciftci, H., Er, C., 2015. Solid phase extraction of lithium ions from water samples using K-birnessite with layer-structure material form (KBRLSM). Desal. Water Treat. 56 (1), 216–222. https://doi.org/10.1080/19443994.2014.932712.

Wang, S.L., Hseu, R.J., Chang, R.R., Chiang, P.N., Chen, J.H., Tzou, Y.M., 2006. Adsorption and thermal desorption of Cr(VI) on Li/Al layered double hydroxide. Coll. Sur. A Phys. Eng. Asp. 277 (1-3), 8–14. https://doi.org/10.1016/j.colsurfa.2005.10.073.

Dewulf, J.o., Van der Vorst, G., Denturck, K., Van Langenhove, H., Ghyoot, W., Tytgat, J., Vandeputte, K., 2010. Recycling rechargeable lithium ion batteries: Critical analysis of natural resource savings. Res. Con. Recy. 54 (4), 229–234. https://doi.org/10.1016/j.resconrec.2009.08.004.

Kang, D.H.P., Chen, M., Ogunseitan, O.A., 2013. Potential environmental and human health impacts of rechargeable lithium batteries in electronic waste. Environ. Sci. Technol 47 (10), 5495–5503. https://doi.org/10.1021/es400614y.

Xu, J., Thomas, H.R., Francis, R.W., Lum, K.R., Wang, J., Liang, B.O., 2008. A review of processes and technologies for the recycling of lithium-ion secondary batteries. J. Pow. Sour. 177 (2), 512–527. https://doi.org/10.1016/j.jpowsour.2007.11.074.

Nikhil C.P., Nair K.K., Usha K.A. (2018). Performance comparison of macromolecular assisted and immobilized low pressure membranes in the removal of toxic metals. Mat. Res. Exp., https://doi.org/10.1088/2053-1591/aad273.

Jha, R., Rao, M.D., Meshram, A., Verma, H.R., Singh, K.K., 2020. Potential of polymer inclusion membrane process for selective recovery of metal values from waste printed circuit boards: a review. J. Clean. Product. 265, 121621. https://doi.org/10.1016/j.jclepro.2020.121621.

Nikhil, C.P., Mothi, K.M., 2020. Tailor made polyelectrolyte multilayers for the removal of obidoxime from water in microfiltration process. Mem. Mem. Technol. 2 (2), 132–147. https://doi.org/10.1134/S2517751620020031.

Chandra, P.N., Usha, K., 2021. Removal of atrazine herbicide from water by polyelectrolyte multilayer membranes. Mat. Today Product. 41, 622–627. https://doi.org/10.1016/j.matpr.2020.05.263.

Cruz, B.H., DõÃaz-Cruz, J.Ã.M., ArinÃo, C., Esteban, M., 2000. Heavy metal binding by tannic acid: a voltammetric study. Electroanalysis. https://doi.org/10.1002/1521-4109(200010)12:14%3C1130::AID-ELAN1130%3E3.0.CO;2-7.

Sorenson, W.R., Sullivan, D., 2007. Determination of campesterol, stigmasterol, and beta-sitosterol in saw palmetto raw materials and dietary supplements by gas chromatography: collaborative study. J AOAC Int. https://www.ncbi.nlm.nih.gov/pmc/articles/PMC2614112/.

Zeng, W., Chen, Y., Cui, H., Wu, F., Zhu, Y., Fritz, J.S., 2006. Single-column method of ion chromatography for the determination of common cations and some transition metals. J. Chro. A 1118 (1), 68–72. https://doi.org/10.1016/j.chroma.2006.01.065.

Chandra, P.N., Mohan, M.K., 2020. Transport studies of ionic solutes through chitosan/chondroitin sulfate A (CHI/CS) polyelectrolyte multilayer membranes. Nano Exp. 1 (2), 020004. https://doi.org/10.1088/2632-959X/ab9fd3.

Baker, L.A., 2011. Can urban P conservation help to prevent the brown devolution? Chemosphere 84 (6), 779–784. https://doi.org/10.1016/j.chemosphere.2011.03.026.

Vinogradova, O.I., Andrienko, D., Lulevich, V.V., Nordschild, S., Sukhorukov, G.B., 2004. Young's modulus of polyelectrolyte multilayers from microcapsule swelling. Macromolecules 37 (3), 1113–1117. https://doi.org/10.1021/ma0350213.

Kavitha V.U., Kandasubramanian B. (2020). Tannins for wastewater treatment. SN Appl. Sci., https://doi.org/10.1007/s42452-020-2879-9.

Kraal, P., Jansen, B., Nierop, K.G.J., Verstraten, J.M., 2006. Copper complexation by tannic acid in aqueous solution. Chemosphere 65 (11), 2193–2198. https://doi.org/10.1016/j.chemosphere.2006.05.058.

Fu, Z., Chen, R., 2019. Study of complexes of tannic acid with Fe(III) and Fe(II). J. Anal. Methods Chem. 2019, 1–6. https://doi.org/10.1155/2019/3894571.

Gupta, U., Singh, VivekK., Kumar, V., Khajuria, Y., 2014. Spectroscopic studies of cholesterol: fourier transform infra-red and vibrational frequency analysis. Mat. Foc. 3 (3), 211–217. https://doi.org/10.1166/mat.2014.1161.

Palombo, F., Shen, H., Benguigui, L.E.S., Kazarian, S.G., Upmacis, R.K., 2009. Micro ATR-FTIR spectroscopic imaging of atherosclerosis: an investigation of the contribution of inducible nitric oxide synthase to lesion composition in ApoE-null mice. Analyst 134 (6), 1107. https://doi.org/10.1039/b821425e.

Jaswal B.B.S., Kumar V., Swart H.C., Sharma J., Rai P.K., Singh V.K. (2015). Multi-spectroscopic analysis of cholesterol gallstone using TOF-SIMS, FTIR and UV–Vis spectroscopy. App. Phy. B, https://doi.org/10.1007/s00340-015-6200-3.

Goossens, K., Nockemann, P., Driesen, K., Goderis, B., Görller-Walrand, C., Van Hecke, K., Van Meervelt, L., Pouzet, E., Binnemans, K., Cardinaels, T., 2008. Imidazolium ionic liquid crystals with pendant mesogenic groups. Chem. Mat. 20 (1), 157–168. https://doi.org/10.1021/cm702321c.

Metzler, R., Jeon, J.H., Cherstvy, A.G., 2016. Non-Brownian diffusion in lipid membranes: Experiments and simulations. Biochim. Biophys. Acta. https://doi.org/10.1016/j.bbamem. 2016.01.022.

Bou Saab, H., Fouchard, S., Boulanger, A., Llopiz, P., Neunlist, S., 2013. Luffa cylindrica and phytosterols bioconversion: From shake flask to jar bioreactor. J. Ind. Mic 40 (11), 1315–1320. https://doi.org/10.1007/s10295-013-1315-1.

Tan, X., Li, M., Cai, P., Luo, L., Zou, X., 2005. An amperometric cholesterol biosensor based on multiwalled carbon nanotubes and organically modified solgel/ chitosan hybrid composite film. Anal. Biochem. 337 (1), 111–120. https://doi.org/10.1016/j.ab.2004.10.040.

Sylwia M., Amanda G., Michał Z., Dominika D., (2019). Adam, C. Investigations on the properties and performance of mixed-matrix polyethersulfone membranes modified with halloysite nanotubes. Polymers, https://dx.doi.org/10.3390%2Fpolym11040671.

Wang, Y., Chen, S.i., Zhao, S., Chen, Q., Zhang, J., 2020. Interfacial coordination assembly of tannic acid with metal ions on three-dimensional nickel hydroxide nanowalls for efficient water splitting. J. Mater. Chem. A 8 (31), 15845–15852. https://doi.org/10.1039/D0TA02229B.

Dong, Z., Jiang, M.-Y., Shi, J., Zheng, M.-M., Huang, F.-H., 2019. Preparation of immobilized lipase based on hollow mesoporous silica spheres and its application in ester synthesis. Molecules 24 (3), 395. https://doi.org/10.3390/molecules24030395.

Zhang, Y.-M., You, X.-M., Yao, H., Guo, Y., Zhang, P., Shi, B.-B., Liu, J., Lin, Q.i., Wei, T.-B., 2014. A silver-induced metal-organic gel based on biscarboxyl-functionalised benzimidazole derivative: stimuli responsive and dye sorption. Supramol. Chem. 26 (1), 39–47. https://doi.org/10.1080/10610278.2013.822968.

Reddad Z., Gerente C., Andres Y., Cloirec P. (2002). Adsorption of several metal ions onto a low cost biosorbent: Kinetic and equilibrium studies. Env. Sci. and Tech., https://doi.org/10.1021/es0102989.

Hu, M.-X., Yang, Q., Xu, Z.-K., 2006. Enhancing the hydrophilicity of polypropylene microporous membranes by the grafting of 2-hydroxyethyl methacrylate via a synergistic effect of photoinitiators. J. Mem. Sci. 285 (1-2), 196–205. https://doi.org/10.1016/j.memsci.2006.08.023.

Huang, J.-H., Zeng, G.-M., Fang, Y.-Y., Qu, Y.-H., Li, X., 2009. Removal of cadmium ions using micellar-enhanced ultrafiltration with mixed anionic-nonionic surfactants. J. Mem. Sci. 326 (2), 303–309. https://doi.org/10.1016/j.memsci.2008.10.013.

Rivas, B.L., Moreno-Villoslada, I., 1998. Binding of Cd^{2+} and Na^{+} Ions by Poly(sodium 4-styrenesulfonate) analyzed by ultrafiltration and its relation with the counter ion condensation theory. J. Phys. Chem. B 102 (36), 6994–6999. https://doi.org/10.1021/jp980941m.

Sablani, S.S., Goosen, MFA, Al-Belushi, R., Wilf, M., 2001. Concentration polarization in ultrafiltration and reverse osmosis: a critical review. Desalination 141 (3), 269–289. https://doi.org/10.1016/S0011-9164(01)85005-0.

Qdais, H.A., Moussa, H., 2004. Removal of heavy metals from wastewater by membrane processes: a comparative study. Desalination 164 (2), 105–110. https://doi.org/10.1016/S0011-9164(04)00169-9.

Ilyas, S., Abtahi, S.M., Akkilic, N., Roesink, H.D.W., de Vos, W.M., 2017. Weak polyelectrolyte multilayers as tunable separation layers for micro-pollutant removal by hollow fiber nanofiltration membranes. J. Mem. Sci. 537, 220–228. https://doi.org/10.1016/j.memsci.2017.05.027.

Petelska, A.D., Figaszewski, Z.A., 2000. Effect of pH on the interfacial tension of lipid bilayer membrane. Biophys. J. 78 (2), 812–817. https://doi.org/10.1016/S0006-3495(00)76638-0.

Zeng, J., Ye, H., Hu, Z., 2009. Application of the hybrid complexation–ultrafiltration process for metal ion removal from aqueous solutions. J. Haz. Mat. 161 (2-3), 1491–1498. https://doi.org/10.1016/j.jhazmat.2008.04.123.

Wu, H., Zou, X., Wu, X.-L., 2020. Nanoconstruction and nanoeffect of phosphate-based cathode materials for advanced sodium-ion batteries. Nano Future 4 (4), 042001. https://doi.org/10.1088/2399-1984/abc103.

Üçer A., Uyanık A., Çay S., Özkan Y. (2005). Immobilisation of tannic acid onto activated carbon to improve Fe(III) adsorption. Sep. and Pur. Tech., https://doi.org/10.1016/ j.seppur. 2004.11.011.

Wen, X., Peihua, M., Chaoliang, Z., Qiong, H., Xiaochuan, D., 2006. Preliminary study on recovering lithium chloride from lithium-containing waters by nanofiltration. Sep. and Pur. Tech. 49 (3), 230–236. https://doi.org/10.1016/j.seppur.2005.10.004.

Chung, K., Lee, J., Kim, W., Kim, S.B., Cho, K.Y., 2008. Inorganic adsorbent containing polymeric membrane reservoir for the recovery of lithium from seawater. J. of Mem. Sci. 325 (2), 503–508. https://doi.org/10.1016/j.memsci.2008.09.041.

Samuel, B., Kazuharu, Y., Syouhei, N., Müşerref, A., Nalan, K., 2017. Application of bipolar membrane electrodialysis (BMED) for simultaneous separation and recovery of boron and lithium from aqueous solutions. Desalination. 424, 37–44. https://doi.org/10.1016/j.desal.2017.09.029.

Wenhui, S., Xiaoyue, L., Chenzeng, Y., Xiehong, C., Congjie, G., Jiangnan, S., 2019. Efficient lithium extraction by membrane capacitive deionization incorporated with monovalent selective cation exchange membrane. Sep. and Pur. Tech. 210, 885–890. https://doi.org/10.1016/j.seppur.2018.09.006.

Mohammad, K., Arne, V., Emile, R.C., Arnout, D., 2020. Crown ether containing polyelectrolyte multilayer membranes for lithium recovery. J. of Mem. Sci. 595,. https://doi.org/10.1016/j.memsci.2019.117432 117432.

Ounissi, T., Dammak, L., Fauvarque, J.F., Hmida, E.S.B.H., 2021. Ecofriendly lithium-sodium separation by diffusion processes using lithium composite membrane. Sep. and Pur. Tech. 275,. https://doi.org/10.1016/j.seppur.2021.119134 119134.

Yakubu, A.J., Ezgi, Ç., Deniz, İ., Esra, A., Nalan, K., 2021. Comparison of two electrodialysis stacks having different ion exchange and bipolar membranes for simultaneous separation of boron and lithium from aqueous solution. Desalination. 500,. https://doi.org/10.1016/j.desal.2020.114850 114850.